This is an extended version of the paper presented in SEE7 conference, peer-reviewed again and approved by the JSEE editorial board.

Effect of Flange Width of Vertical Link Beam on Cyclic Behavior of Chevron Braced Steel Frames

Seyed Mehdi Zahrai[1*] and Amir Parsa[2]

1. Professor, School of Civil Engineering, College of Engineering, the University of Tehran, Tehran, Iran, * Corresponding Author; email: mzahrai@ut.ac.ir
2. M.Sc. Student, School of Civil Engineering, the University of Tehran, Tehran, Iran

Received: 27/02/2016
Accepted: 09/08/2016

ABSTRACT

Among the passive dampers, using Vertical Link Beam (VLB) is one of the most effective and simplest methods, while not embedded in the floor they can be easily replaced after earthquakes. These dampers dissipate a major part of the input energy resulting in a minimized damage of the main structural components of system. This paper presents a numerical study on the impact of flange width of VLB on cyclic performance of chevron braced steel frames. Despite most previous research projects in which wide-flange I sections were considered for the VLB and the length of VLB was studied, here, the objective is to investigate the possibility of using narrower flange. Verification has been made on the basis of the experimental results from the IPE160 model. By changing the flange width, the cyclic behavior has been investigated. The results show that while the vertical link beam has sufficient lateral support, in spite of the flange width reduction, stable hysteretic cycles still form accompanied with considerable energy dissipation. Based on the hysteretic curves, using modification of the narrower flange section, the shear force at last cycle increased about 20.74% and 16.17% in IPE160 VLBs with a half and quarter flange width respectively, and the proportion of VLB in plastic energy dissipation increased from 78.9% to 90.4% in half flange VLB and from 74.2% to 90.9% in quarter flange VLB only by this simple modification, showing an increase in ductility of the system

Keywords:
Vertical link beam; Chevron bracing; Eccentrically braced frame; Flange width; Passive control

1. Introduction

Shear Panel System, SPS, or Vertical Link Beam, VLB, is a passive control method located vertically between the joint of two chevron braces and the flange of the floor beam as shown in Figure (1). H-shaped or IPB sections with wide flanges are often used as a shear panel. Appearance of these pieces is like a short beam linking chevron braces to the beam (Figure 1). This system has stable hysteresis curves such that without causing any strength degradation or stress concentration, it can uniformly dissipate energy. SPS has high ductility in addition to having considerable lateral stiffness. In this system, because of suitable ductility, limited relative floor displacements and maximum displacements of buildings cannot easily cause damage in the building. Unlike Eccentrically Brace Frames, EBFs, SPS as a ductile fuse is not inside of the floor slab and if connected to the main beam with bolts, it is easily exchangeable. Just by changing SPS if needed, the structure can still sustain future earthquakes. Another main benefit of this system is its easy use in seismic retrofit of existing buildings. Overall, using SPS as

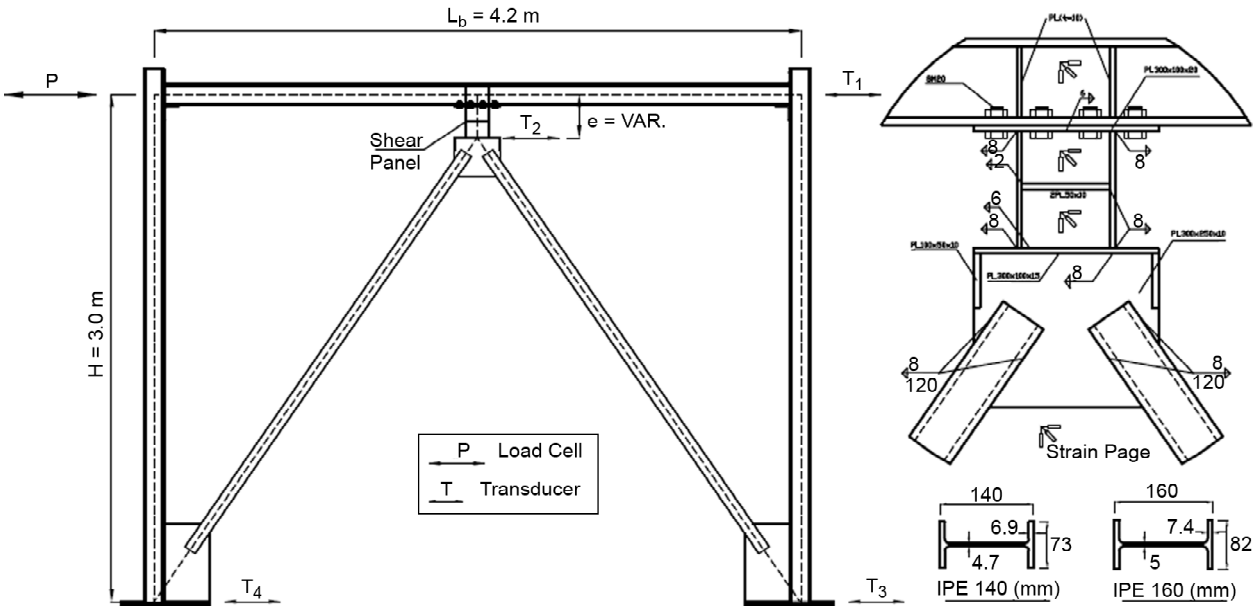

Figure 1. Vertical link beam or shear panel system.

an efficient method, with little expense in terms of design, construction and exchange looks promising.

To experimentally study the cyclic behavior of SPS, Bouwkamp and Vetr [1] tested a full-scale SPS frame with three stories and three spans of 5 m. Columns were arranged at minor axes to assign maximum story shear to links. Method of loading was displacement control as well as controlling the ratio of load applied to levels respectively 1/3, 2/3 and 1 at the first to third stories. Almost all shear panel systems reached web failure synchronized at 15-20 mm. After failure of links, general and local stiffness of frame decreased seriously, but because of hardening, the strain in the links of the whole system continuously increased. Almost 90% of imposed energy was dissipated by SPS showing that all inelastic deformations occurred in the links, without other members suffering large strains. Because short shear panels permit plastic deformations and prevent buckling, moment and shear resistance can reach their maximum capacity in the link plastic zone with combination of kinematic and isotropic hardenings [1].

To find out if hollow structural sections instead of wide-flange or I-shaped ones can also effectively dissipate energy as EBF links, Wiliams and Albermani [2] performed a quite extensive series of tests with various thicknesses of both single and double diaphragm plates on Square Hollow Section (SHS) with 100 mm dimension. No buckling or failure occurred at cap beam displacement of up to 30 mm and all specimens had open stable hysteresis loops until 40 mm. Thinner diaphragms obtained a local ductility of 20, while the ductility of thicker ones was between 10 and 15. In all cases, the global ductility of frames was around 8. Diaphragms withstood maximum shear strain around 11.8 to 24.2% without failure.

Berman and Bruneau [3] also conducted an experimental and analytical investigation to use hollow rectangular cross-sections instead of wide-flange or I-shaped ones as SPS in EBFs. These specimens in contrast to I-shaped cross-sections do not essentially require lateral bracing. Very short links have large stiffness, and thus, large base shear forces should be provided. Therefore, a bit longer link, still maintaining shear behavior was used. The link was designed in a way that flange or web buckling would not occur. Compactness of flange and web in addition to stiffener spacing was checked according to the AISC Specifications, and the tests proved that these specifications were efficient. The yield drift and the corresponding base shear were identified as 0.37% and 668 kN while maximum drift and base shear were 2.3% and 1009 kN respectively. The yield rotation and link shear at yield were 0.014 rad and 490 kN while the maximum rotation and link shear were 0.151 rad and 740 kN

respectively. Fracture initiated in the heat-affected-zone adjacent to the fillet weld used to connect the stiffener to the flange [3].

Zahrai and Moslehi Tabar [4] conducted a numerical study on shear panel system that acts as a ductile link beam connecting braces to the floor beam. The study was about key issues influencing cyclic behavior of frames braced by SPSs, like Cross-sectional properties of SPS and link length. The results indicated that shear panel length significantly affects cyclic performance of this system. For the studied cases, the use of shorter link increased energy dissipation capacity of the braced frame by 50% compared with the similar braced frame having longer link and web stiffeners provided in the shear panel, and improved the behavior of the shear panel and thus the braced frame, especially for larger deformations. Considering drift limitations for the frame, the energy dissipation capability of the SPS can be improved by increasing the web depth and web thickness of the shear panel, or by reducing the shear panel length. Finally, they presented a mathematical model to evaluate lateral stiffness of the braced frames having SPS [4].

De Matteis et al. [5] conducted an extensive series of experimental and numerical studies testing the behavior of aluminum alloy stiffened shear panels as a passive seismic device being able to dissipate a large amount of energy. A good agreement was observed between experimental and numerical results to model the behavior of the device [5]. Ozhendekci and Ozhendekci [6] designed 420 EBFs with shear links, 105 EBFs with intermediate links, and 105 EBFs with moment links and performed inelastic dynamic analyses using DRAIN-2DX to investigate the effects of the geometry selection on the seismic behaviors and weights of the frames.

Hossain et al. [7] used a decomposed kinematic hardening rule to simulate nonlinear material behavior in modeling Yield Shear Panel Device, YSPD as a small, inexpensive and easy to install device. The basic point was to concentrate the inevitable structural damages to YSPDs and hence keeping the main structural components intact. Based on their findings, the simplicity of YSPD allows the damaged devices to be replaced by the new ones without any major structural reconstruction [7]. Hossain et al. [8] used a theoretical approach to predict the initial stiffness of (YSPD) compared with both experiments and developed FE models analyzed by ANSYS. YSPD relies on the in-plane shear deformation of a thin diaphragm steel plate welded inside a Square Hollow Section (SHS). SHS as a boundary element causes tensile strips to be formed and the tension field to be developed following the post-buckling of the thin diaphragm plate. Because of large displacement in the diaphragm plate, most earthquake energy would be dissipated by plastic deformation [8].

In order to carefully understand the link behavior at different levels of nonlinear deformations, Zahrai and Moslehi Tabar [9] developed an extended mathematical model for evaluation of lateral stiffness of braced frames having SPS. They proposed a mathematical expression to select the geometric properties of the SPS regarding the desired ductility and found that, the ultimate plastic lateral deformation is directly proportional to the link length, and a deteriorating coefficient accounting for the tri-axial stress effect. According to their proposed relation, the SPS geometric properties may be pre-selected regarding the desired plastic deformation [9].

In another research using aluminum SPS, Rai et al. [10] conducted a shake table study of a single-bay two-story 1:12 reduced scale model of a braced frame with aluminum shear-link to evaluate the performance of shear-links as energy dissipation devices. The test indicated that the frame attracted about 41-64% less base shear compared to ordinary CBF for varying PGA levels of the ground motions. Significant amount of energy was absorbed by aluminum shear-links leading to satisfactory response up to the scaled PGA of 1.7 g, while the CBF frame could not survive the scaled PGA of 0.8 g [10].

Zahrai [11] experimentally investigated the lateral behavior and related benefits of the Shear Panel System, SPS, with narrow-flange link beams in chevron braced simple steel frames. For this purpose, five specimens with IPE (narrow-flange I section) shear panels were examined. All of the specimens showed high ductility and dissipated almost all input energy imposed to the structure. For example, maximum SPS shear distortion of 0.128-0.156 rad, overall ductility of 5.3-7.2, response modification factor of 7.1-11.2, and finally, maximum equivalent viscous damping ratio of 35.5-40.2% in the last loading cycle corresponding to an average

damping ratio of 26.7-30.6% were obtained. It was also shown that the beam, columns and braces remained elastic as expected. Besides, the reduction factors of the specimens were computed between 10 and 16. Average equivalent viscous damping ratios in the inelastic cycles reached 26.7-30.6% showing a high dissipation of the cyclic energy by these pieces. Short shear panels having shear behavior showed better performances than long ones with flexural behavior [11].

In the most research projects mentioned above, the wide flange sections have been used, and just few researchers recently considered the narrow flange section or IPE section as a vertical link beam, in which they had acceptable results and stable behavior with desired energy dissipation. In this study, the objective is to investigate the effect of decreasing flange width on cyclic behavior. Therefore, the flange width is first increased compared to the IPE section, then the width will be reduced to a half and a quarter of the original size all subjected to the cyclic loads to see if these changes can improve or damage the cyclic performance of this system.

2. Determination of Reduction Factor

To determine the reduction factor or response modification factor, the following formula is used:

$$R_w = R_\mu \times \Omega_0 \times Y \tag{1}$$

In which, R_w is the reduction factor of structure (for allowable stress design method), R_μ is the real reduction factor due to ductility, Ω_0 is the overstrength coefficient and Y is the allowable stress factor. Note that for R_u (for limit state or Load and Resistance Factor Design, LRFD method used in the new edition of seismic design code, Standard 2800 Ver4), R_w must be divided by 1.4 [12]. R_μ is a function of structure lateral period, T, total ductility factor of structure, μ, and type of the soil. Ω_0, as a result of redistribution of internal forces, strain hardening and influence of strain rate is related to the factors such as type of structural system, shape of the structure, number of stories. Y, allowable stress factor is used for considering differences in the pattern of codes in designing with the limit state method or the permissible-stress method [13]. The total ductility factor of structure, μ, is equal to the ratio of maximum displacement, Δ_{max}, to equivalent yield displacement, Δ_y.

Ω_0 is the storage resistance between the first real level of yielding, C_y, and the first level of considerable yielding, C_s, that their quantities are obtained from force-displacement curves of the frames as typically shown in Figure (2).

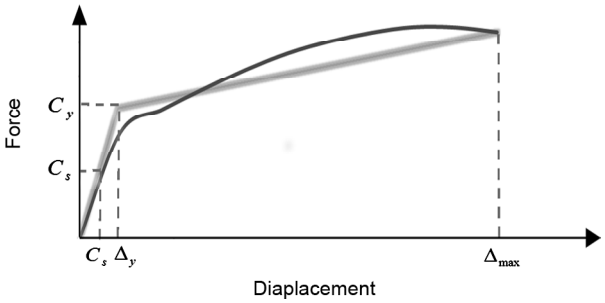

Figure 2. Parameters used in calculation of ductility, overstrength factor and allowable reduction factor.

$$\Omega_0 = \frac{C_y}{C_s} \tag{2}$$

Y is equal to the proportion of the first level of considerable yielding, C_s, and the related level of the design force, C_w.

$$Y = \frac{C_s}{C_w} \tag{3}$$

According to the AISC code, this factor is equal to:

$$Y = \frac{ZF_y}{S(0.6F_y \times \frac{4}{3})} = \frac{1.25Z}{S} \tag{4}$$

where Z and S are plastic and elastic section modulus respectively, and the geometrical parameters of the section of VLB used in the calculation are shown in Figure (3).

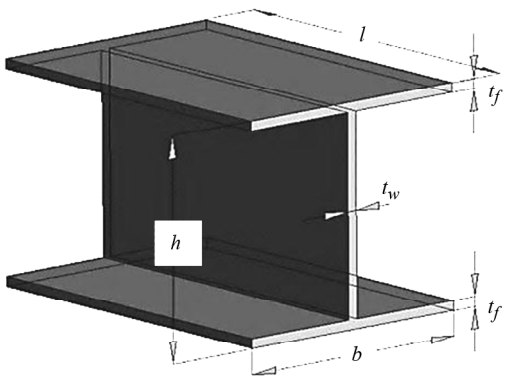

Figure 3. Geometrical parameters of the section of VLB.

3. Numerical Study

In this paper, the models are analyzed by developed finite element software, ABAQUS. The 3D shell elements with four nodes and type S4R are chosen. The reason for using the shell elements in modeling, is that the thickness of steel sheets is negligible related to their other dimensions.

The model has one floor and is a single-bay frame, since designing a single floor and single-bay frame under real loads usually results in small sections for structure elements, it was decided that by presuming details of shear panel, other elements would be designed proportional to the shear capacity of the shear panels. In Table (1), geometry details of the frame and shear panels are given.

The welded joints are also used for all relevant joints. Hinge connection is used for the beam-to-column connection.

4. Lateral Loading

The quasi-static loading protocol used here was developed based on the guidelines presented in Applied Technology Council 1992 (ATC-24) [14]. In order to assess a reasonable value of yielding displacement (Δ_y), force-control load history was applied to the test frame before the appearance of yielding on the vertical link beam as shown in Figure (4). According to Figure (4), the yield displacement

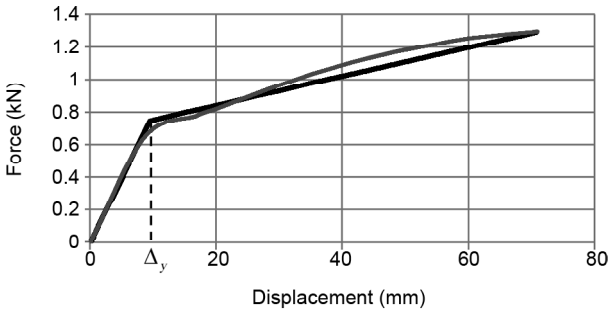

Figure 4. Pushover curve to determine yielding displacement (Δ_y) of vertical link beam.

of vertical link beam is about 8 mm [11].

According to ATC-24 loading protocol, lateral loading was applied using displacement control: three cycles at each of 0.125, 0.25, 0.5, 1, 2, and , and two cycles from to specimen rupture as shown in Figure (5) [14].

5. Numerical Modeling and Results of Verification

As mentioned before, Zahrai [11] experimentally studied five specimens with IPE shear panels. First, to verify the numerical model of the first tested specimen (SPS1) as presented in Figure (6) is modeled. The material properties of the steel frame used in the model are according to the conducted tests as presented in Table (2).

In this tested sample, the IPE160 section is used

Table 1. Geometric properties of the steel frame having vertical link beam.

Members of Frame	Vertical Link Beam	Brace	Beam	Column
Section	IPE160	2UNP80	IPB140	IPB120
Length (cm)	20	345	420	300

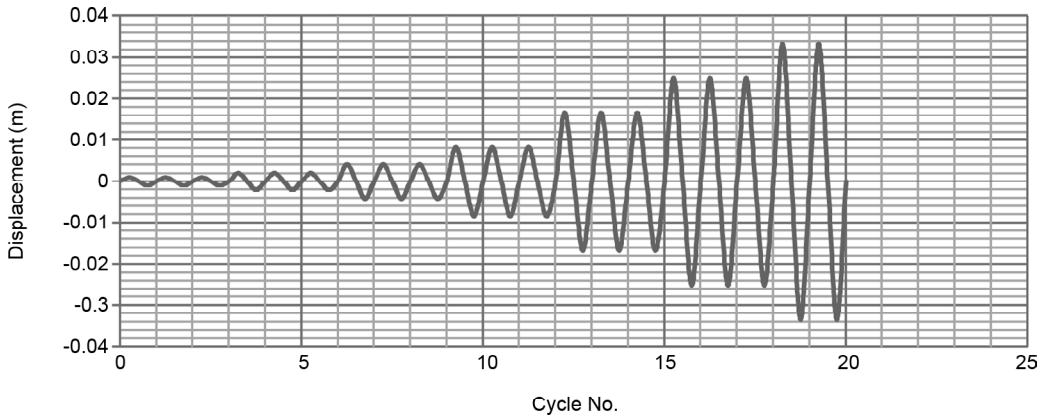

Figure 5. Displacement cycles applied according to ATC-24 1992 [14].

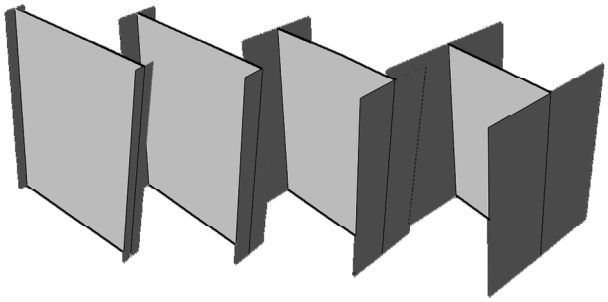

Figure 6. VLBs with various flange width.

Table 2. Material properties of the steel frame components.

Members of Frame	$F_u(\frac{kg}{cm^2})$	$F_y(\frac{kg}{cm^2})$
Vertical Link Beam	4200	2800
Other Members	3700	2400

as a link beam with web stiffeners in the middle height at both sides as shown in Figure (7). Weld connection is used for all members, and since in the laboratory no rupture or crack was observed in the connetion [11], the separated parts in the finite element model are merged together presuming there is no rupture or crack in the model.

As mentioned above, the connection between column and beam is hinge. Like experimental work, the columns are hinged to the ground in the finite element model. To prevent out-of-plane movement of the frame, some number-10 bars were used to laterally anchor beam upper flange. According to Figure (7), these anchor bars were installed on both sides of the frame and at specified distances in the experiment; and therefore, the out-of-plane movement of the frame is prevented in the finite element model.

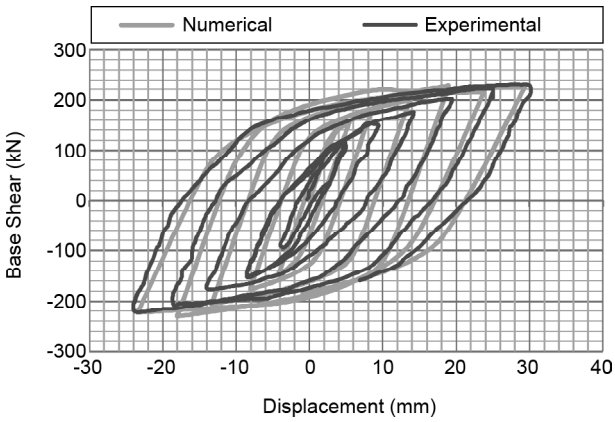

Figure 8. Good agreement between numerical and experimental hysteresis curves.

According to the cyclic load applied to the model, the hysteresis curve (Figure 8) can show the behavior, energy dissipation and stiffness of the system. As shown in Figure (8), two cases have roughly identical behavior. The numerical model becomes a little stiffer and the base shear also increases due to the rigidity of some joints and negligible little cracks of welding in modeling process.

In Table (3), the base shear at each cycle is presented where a negligible difference between experimental and numerical base shear is shown. The average error is about 6.6%. As mentioned above, finite element model shows a little more stiffness compared to the experimental model, hence in the initial cycles base shear in finite element

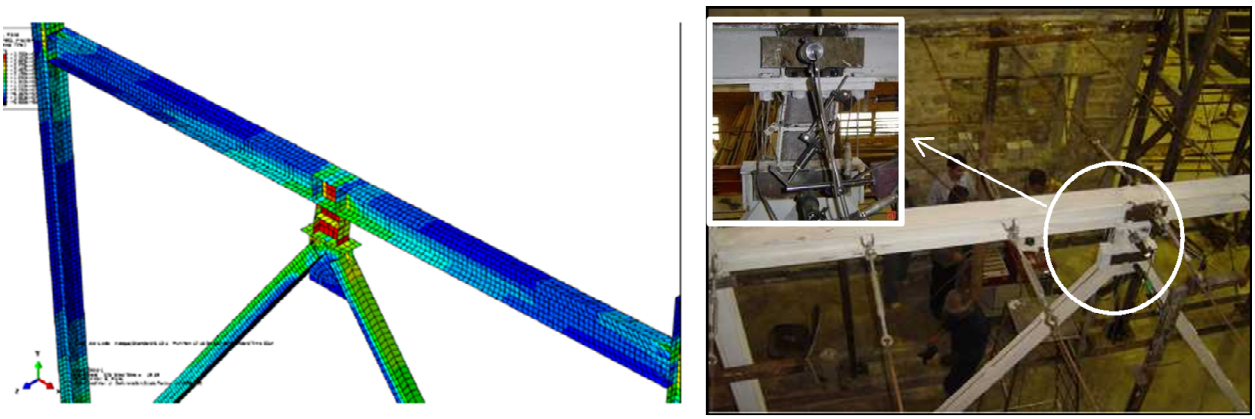

(a) (b)

Figure 7. (a) Specimen with IPE160 shear panels modeled in ABAQUS (b) Specimen with IPE160 shear panels tested in structural laboratory of the Building and Housing Research Center in Tehran, Iran [14].

Table 3. The difference between experimental and numerical base shears at maximum displacement of cycles.

Displacement (mm)	Experimental Base Shear (kN)	Numerical Base Shear (kN)	Percent Error (%)
8	152.68	171.01	12.00
14	175.53	199.17	13.47
19	201.70	227.61	12.85
22	221.99	214.32	3.45
27	229.38	225.20	1.82
Average			**6.61**

model is more than those in experimental model, but in the last cycles this difference is reduced.

One of the important factors is the amount of energy dissipation. The maximum energy dissipation occurs in the last cycles. In the experimental study, this energy dissipation was 14.184 kJ, while in numerical model the energy dissipation is 13.961 kJ, thus the error of the energy dissipation was only about 1.56% and this shows the acceptable accuracy of modeling and the presumptions considered in finite element model.

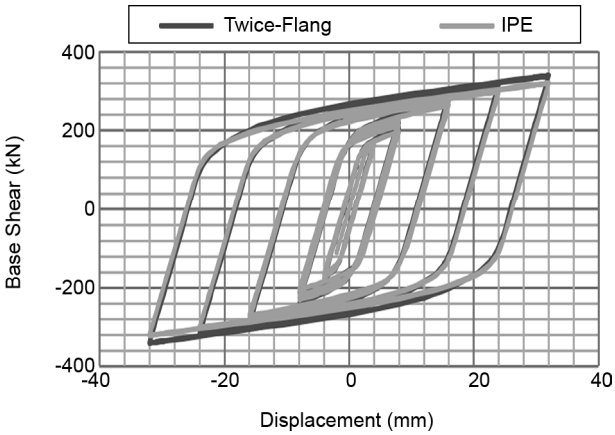

Figure 9. The comparison between hysteretic curves of IPE160 and the section with twice-flange width.

6. Sample Description

As mentioned earlier, the numerical study of the VLB flange role in its cyclic behavior is evaluated in this paper. Therefore, the effect of flange width on damping and energy dissipation of different systems is assessed by changing the width of the VLB flange (Figure 6).

6.1. Samples 1 and 2

This paper first investigates any possible change in cyclic behavior when the flange width of IPE160 becomes greater. Hence, a VLB the same as IPE160 is investigated here but with a wider flange (Figure 9).

Indeed, this looks like a wide flange section used in a form of built-up plate-girder. The result indicates that the hysteretic performance of this model with wider flange is the same as that of the model with IPE160 as a VLB with nearly the same energy dissipation; however, this structure is a little stiffer that can be neglected (Figure 9).

As mentioned before, one of the important operations of VLB is to dissipate the input energy imposed to the systems. As presented in Figure (10), nearly the whole energy is dissipated by VLB.

Both models had the same performance on plastic energy dissipation that could be recognized from Figure (10) where from starting point to about 9th second no plasticity is observed, from second 9 to 11, only VLB yields, and finally from 11th second up to the end, the tiny parts of main structure yield. However, in the worst condition, more than 83.7% in wide flange section model and 87.8% in IPE160 model of the whole energy is dissipated only by VLB.

6.2. Sample 3

Contrary to the previous cases, the effect of the flange width reduction has been attempted to be evaluated. Hence, a VLB like IPE160 but with a half flange width is used. In contrast to previous sample, in this case the behavior of the system changed and after about 15th second a force reduction occurred (Figure 11).

The reason for the reduction of base shear is the buckling of the web of VLB and the resulting instability in VLB. As shown in Figure (12a), this

instability of VLB causes the rotation of the bottom of VLB. As shown in Figure (12b) in modified model, this rotation is prevented by lateral support of VLB.

As shown in Figure (11), by modification of half-flange width model, the hysteretic performance is noticeably improved and the base shear increases about 20.7% at last cycle. An important point that should be considered is that the area under the hysteresis curve and the resulting energy dissipation

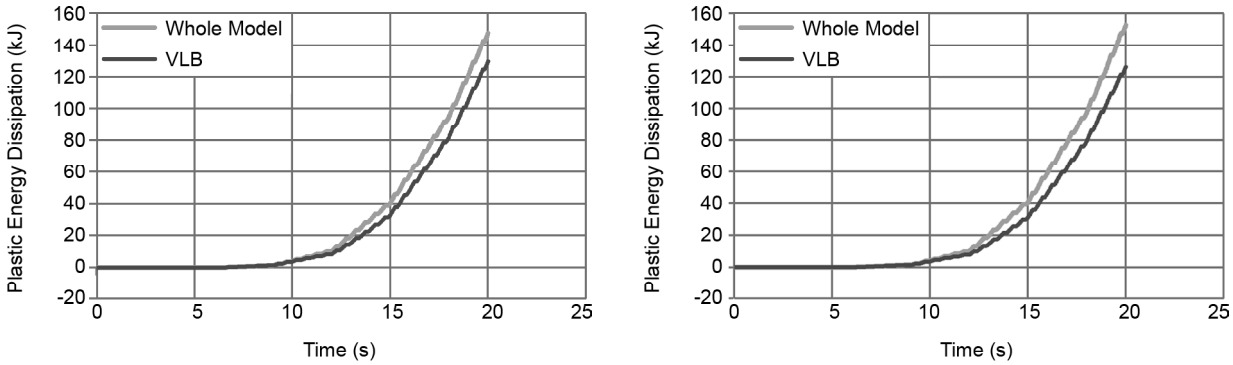

(a) Model with IPE160 as a VLB (b) Model with a Wider Flange Section as a VLB

Figure 10. Share of VLB in plastic energy dissipation of the system.

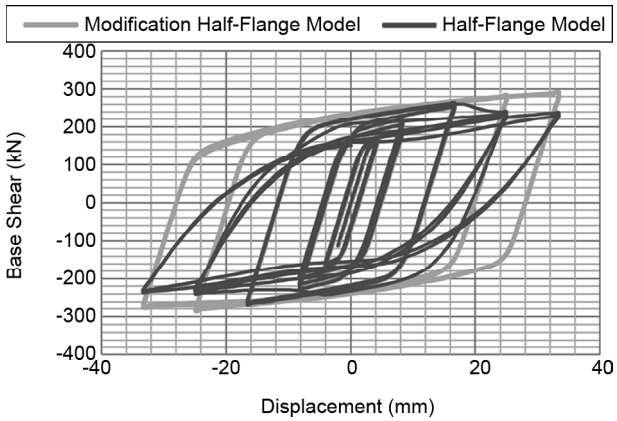

Figure 11. The improvment of hysteretic performance by modification of half-flange width model.

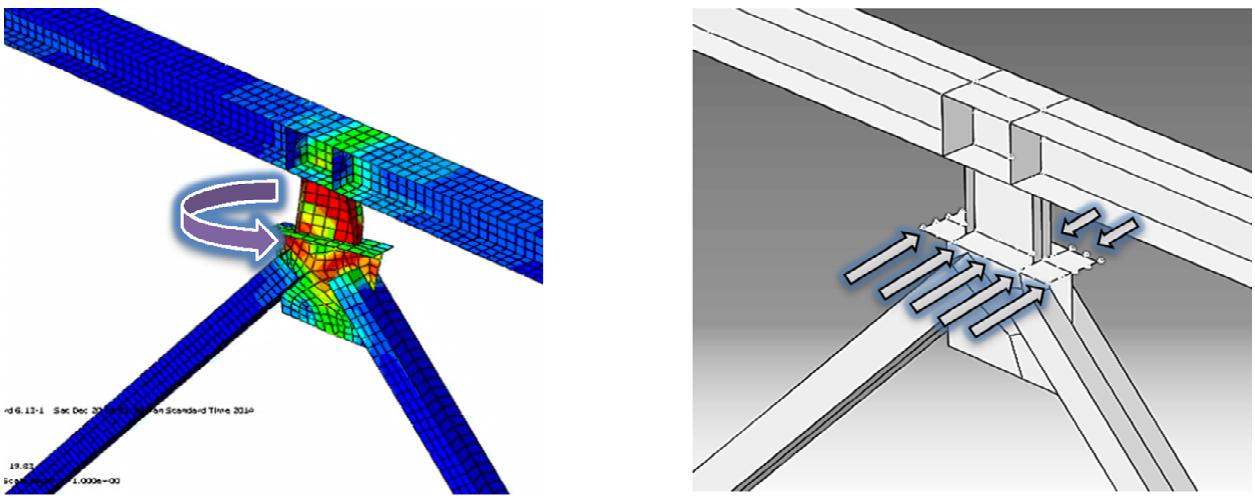

(a) (b)

Figure 12. (a) Instability and rotation in VLB; (b) Modified half-flange width by laterally supporting.

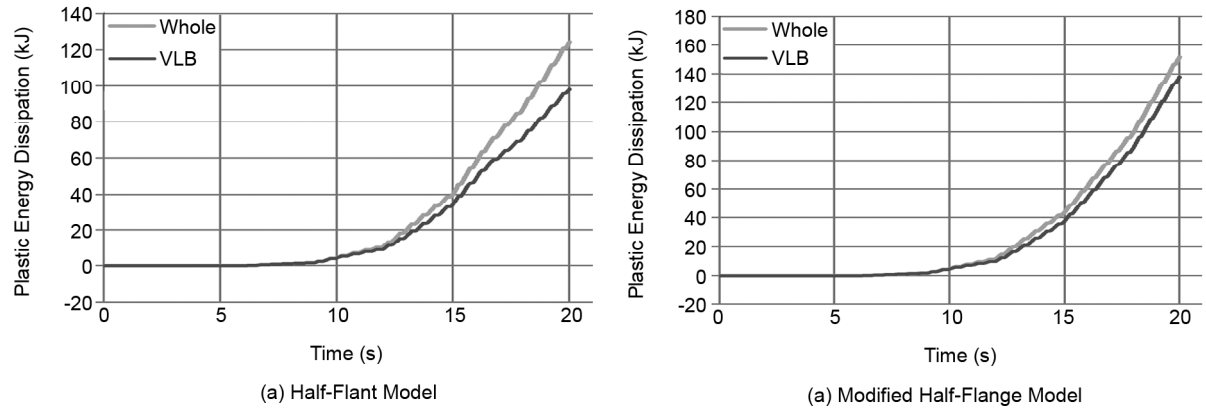

Figure 13. The improvement of VLB performance in dissipating plastic energy in half-flange model.

increase in the modified model. In addition, the proportion of VLB in dissipating plastic energy increases considerably from 78.9% in half-flange model to 90.4% in modified case as observed in Figure (13).

6.3. Sample 4

In this model, like the IPE160 section, a VLB is used but with a quarter of the original flange width. Like the previous cases, in this model, the rotation of VLB is prevented by laterally supporting VLB. On the other hand, the modified model is used in this case.

As presented in Figure (14), the modification in this model is more effective than that in previous model on the hysteretic performance and the base shear increases about 20.7% at last cycle. The reduction on base shear occurs at 15 mm displacement while in the half-flange model this reduction occurs at about 25 mm displacement. This shows that in the recent model (20.5 mm flange width), the modification is more needed. As before by modifying, the rotation of VLB is prevented using lateral support of VLB, and consequently, no global buckling is observed in contrast to the model without lateral supporting. The system remains stable during loading and just negligible local buckling occurs that can be ignored (Figure 15).

Another important point that should be considered is that besides the reduction in base shear at the end of each cycle, in the middle parts of each cycle the reduction is observed. On the other hand, pinching occurs in recent model with no modification. Consequently, the energy dissipation by VLB considerably decreases as shown in Figure (15). But with modification no pinching is observed (Figure 14) and the proportion of VLB in dissipating plastic energy increases considerably from 74.15%

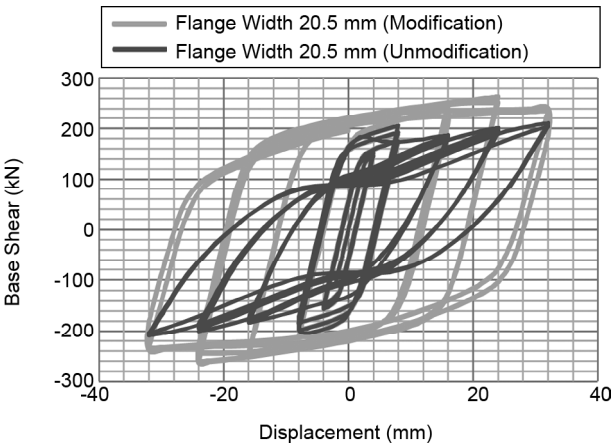

Figure 14. The considerable improvement of hysteretic performance by modification of flange width 20.5 mm model.

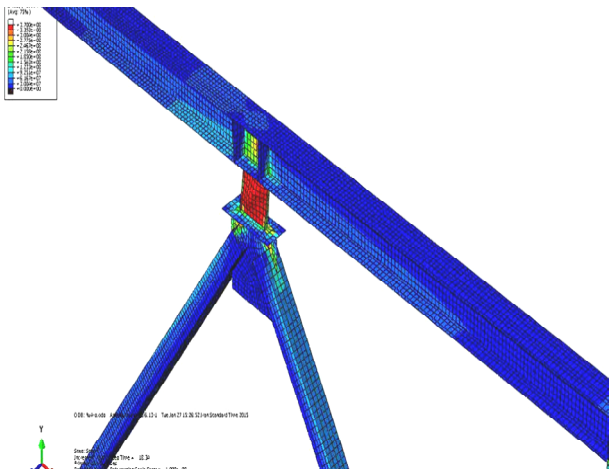

Figure 15. Stability in modified 20.5 mm flange width model with local buckling in the VLB web.

in 20.5 mm flange width model to 90.9% in modified case as shown in Figure (16).

In Figure (17), the hysteretic performance of the last model is compared to that of the first model in which IPE160 is used as a VLB. The results show that in comparison with the previous state, the system stiffness has a reduction, and of course this decrease can be observed only in high displacements (at least 16 mm) and in such regions. However, up to a nearly 3 cm displacement, no global instability can be observed in the system and the damper still truly plays the role of an energy dissipater.

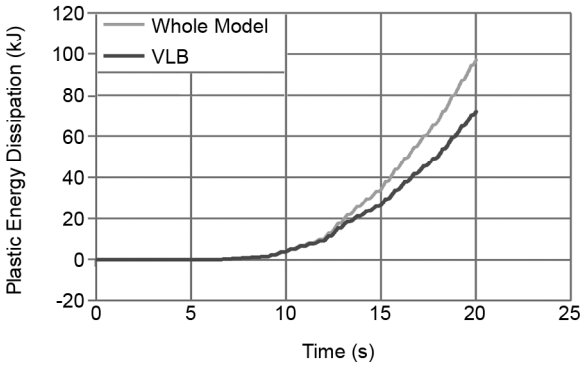

(a) 20.5 mm Flang Width

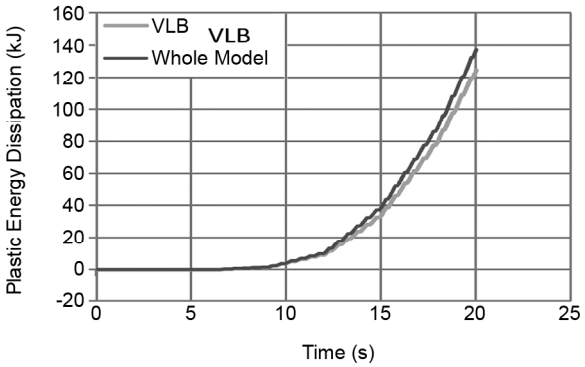

(b) Modified 20.5 mm Flange Width

Figure 16. The improvement of VLB performance in dissipating plastic energy in 20.5 mm flange width model.

7. Reduction Factor

Using Eq. 1 reduction factor of each model is computed as presented in Table (4) where the reduction factor varies between 9.2 and 10.34. As presented in Table (4), reducing the VLB flange width leads to an increase in reduction factor of given frame. In fact, the reduction of the flange width, besides the aforementioned effects, leads to an

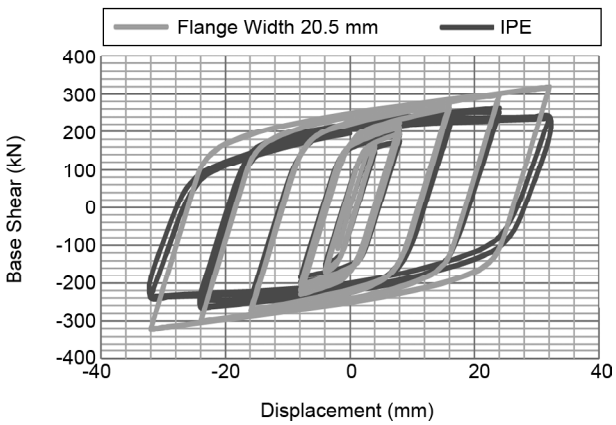

Figure 17. The comparison between hysteretic curves of IPE160 and 20.5 mm flange width model.

Table 4. The difference between experimental and numerical base shears at maximum displacement of cycles.

	IPE160	Half-Flange Model	Flange with 20.5 mm Width Model
$h(cm)$	16.00	16.00	16.00
$t_w(cm)$	0.50	0.50	0.50
$b(cm)$	8.20	4.10	2.05
$t_f(cm)$	0.74	0.74	0.74
$Z(cm)$	121.71	75.41	52.26
$I(cm^4)$	834.63	481.09	304.32
$S(cm^3)$	104.33	60.14	38.04
Y	1.46	1.57	1.72
C_s(kN)	108	106	103.00
C_y(kN)	165	160	150.00
Ω_0	1.53	1.51	1.46
μ	9.29	9.29	9.29
T(s)	0.82	0.82	0.82
Φ	2.64	2.64	2.64
R_μ	4.14	4.14	4.14
$R_w(ASD)$	*9.21*	*9.78*	*10.34*
$R_u(LRFD)$	*6.58*	*6.99*	*7.39*

increase in the ductility of the system and the reduction factors. Because S is too sensitive to the flange width, its reduction increases Y considerably. Although Ω_0 decreases with decreasing the flange width, an increase in Y is more effective and as a result, the reduction factor decreases by reducing the flange width of VLB.

As presented in Table (4), the reduction factor calculated by Eq. (1) used for the design of steel structures is based on Allowable Stress Design (ASD) method. In new seismic design code, i.e. S tandard 2800 Ver. 4 [12], the design shifts to LRFD method and thus the reduction factors are divided by 1.4 as shown in the last row of Table (4).

8. Conclusions

In this paper, the impact of flange width in the VLB was investigated. First of all, the presence of the lateral support becomes important when reducing the flange width and the frame might face a severe decrease in strength and energy dissipation, because a rotation at the bottom of VLB and consequently the instability in system occurs. Thus, in those models a modification was defined in which the rotation of VLB was prevented with out-of-plane bracing of VLB. As a result of this modification, the hysteretic performance was significantly improved for the mentioned models with no major strength degradation; for instance shear force capacity at last cycle increased about 20.74% in half-flange model and 16.17% in 20.5 mm flange width model. The proportion of VLB in plastic energy dissipation increased from 78.93% to 90.40% in half-flange model and from 74.15% to 90.88% in 20.5 mm flange width model using lateral support.

Another privilege that can be noted is that the VLB acts better like a fuse if lateral support is provided and a decrease in flange width occurs leading to less post stiffness due to related local buckling in high displacements (about 15 mm to 16 mm). Below these values of displacement, such an extra width of flange does not affect the cyclic behavior of the structure. On the other hand, by reducing the width of the flange of VLB, the ductility of the system increases and the reduction factor grows up to 10.3 in the 20.5 mm flange width model.

As a matter of fact, the link beam flange acts as a buckling constraint to the system leading to an increase in its critical buckling loading. The investigations indicate that decreasing flange width of VLB up to 20.5 mm does not lead to the global buckling; although, some local buckling was observed in form of the wavy web of the VLB.

References

1. Boukamp, J.G. and Vetr, M.G. (1994) Design of eccentrically braced test frame with vertical shear link. *Proceeding of the 2nd International Conference on Earthquake Resistant Construction and Design*, Berlin, Germany, June.

2. Williams, M.S. and Albermani, F. (2003) Monotonic and cyclic tests on shear diaphragm dissipators for steel frames. *Civil Eng. Res. Bulletin*, **23**, 1-34.

3. Berman, J.W. and Bruneau, M. (2007) Experimental and analytical investigation of tubular links for eccentrically braced frames. *Eng. Struct.*, **29**(8), 1929-1938.

4. Zahrai, S.M. and Moslehi Tabar, A. (2006) Cyclic Behavior of steel Braced frames using shear panel system. *Asian Journal of civil Engineering*, **7**(1), 13-26.

5. De Matteis, G., Formisano, A., Panico, S., and Mazzolani, F.M. (2008) Numerical and experimental analysis of pure aluminum shear panels with welded stiffeners. *Comput. Struct.*, **86**(6), 545-555.

6. Ozhendekci, D. and Ozhendekci, N. (2008) Effects of the frame geometry on the weight and inelastic behavior of eccentrically braced chevron steel frames. *J. Construct. Steel Res.*, **64**(3), 326-343.

7. Hossain, M.R., Ashraf, M., and Albermani, F. (2009) Numerical evaluation of yielding shear panel device: A sustainable technique to minimize structural damages due to earthquakes. *Universitas 21 International Graduate Research Conference*, Melbourne-Brisbane, Australia, November-December, 65-68.

8. Hossain, Md.R, Ashraf, M., and Albermani, F. (2011) Numerical modelling of yielding shear panel

device for passive energy dissipation. *Thin-Wall. Struct.*, **49**(8), 1032-1044.

9. Zahrai, S.M. and Moslehi Tabar, A. (2013) Analytical study on cyclic behavior of chevron braced frames with shearpanel system considering post-yield deformation. *Canadian Journal of Civil Engineering*, **40**(7), 633-643.
10. Rai, D.C., Annam, P.K., and Pradhan, T. (2013) Seismic testing of steel braced frames with aluminum shear yielding dampers. *Eng. Struct.*, **46**, 737-747.
11. Zahrai, S.M. (2015) Cyclic testing of steel braced frames with IPE shear panels. *Steel and Composite Structures*, **19**(5), 1167-1184.
12. BHRC (2014) Iranian code of practice for seismic resistance design of buildings: Standard No. 2800 (4th Version) Building and Housing Research Center.
13. Miranda, E. (1993) Site dependent strength reduction factor. *J. Struct. Eng.*, ASCE, **119**(12), 3503-3519.
14. Applied Technology Council (1992) *Guidelines for Seismic Testing of Components of Steel Structures*. Report ATC-24.